Can the Cyanobacterial Carbon-Concentrating Mechanism Increase Photosynthesis in Crop Species? A Theoretical Analysis[1][W][OPEN]

Justin M. McGrath and Stephen P. Long*

Institute for Genomic Biology (J.M.M.), Department of Crop Sciences (S.P.L.), and Department of Plant Biology (S.P.L.), University of Illinois, Urbana-Champaign, Illinois 61801

Experimental elevation of [CO_2] around C_3 crops in the field has been shown to increase yields by suppressing the Rubisco oxygenase reaction and, in turn, photorespiration. Bioengineering a cyanobacterial carbon-concentrating mechanism (CCM) into C_3 crop species provides a potential means of elevating [CO_2] at Rubisco, thereby decreasing photorespiration and increasing photosynthetic efficiency and yield. The cyanobacterial CCM is an attractive alternative relative to other CCMs, because its features do not require anatomical changes to leaf tissue. However, the potential benefits of engineering the entire CCM into a C_3 leaf are unexamined. Here, a CO_2 and HCO_3^- diffusion-reaction model is developed to examine how components of the cyanobacterial CCM affect leaf light-saturated CO_2 uptake (A_{sat}) and to determine whether a different Rubisco isoform would perform better in a leaf with a cyanobacterial CCM. The results show that the addition of carboxysomes without other CCM components substantially decreases A_{sat} and that the best first step is the addition of HCO_3^- transporters, as a single HCO_3^- transporter increased modeled A_{sat} by 9%. Addition of all major CCM components increased A_{sat} from 24 to 38 μmol m^{-2} s^{-1}. Several Rubisco isoforms were compared in the model, and increasing ribulose bisphosphate regeneration rate will allow for further improvements by using a Rubisco isoform adapted to high [CO_2]. Results from field studies that artificially raise [CO_2] suggest that this 60% increase in A_{sat} could result in a 36% to 60% increase in yield.

C_3 species include the major grain crops rice (*Oryza sativa*) and wheat (*Triticum aestivum*) and overall accounted for approximately 75% of all primary foodstuff production in 2012 (FAOSTAT, 2013). The yield of many crop species has been substantially improved through breeding and agronomy, but advancement in yield has substantially slowed in many of the major C_3 crops in the last decade, suggesting that limits on yield improvement using these techniques are being reached and that other approaches are needed (Long and Ort, 2010; Ray et al., 2012).

One largely unexploited approach would be to improve the efficiency of photosynthesis in these species (Zhu et al., 2010). The photosynthetic enzyme Rubisco catalyzes the reaction of CO_2 with ribulose bisphosphate (RuBP), which eventually forms carbohydrates. However, Rubisco will also react with oxygen as the first step in photorespiration. This reaction is considered wasteful, since energy is consumed to recover RuBP and CO_2 is lost in the process. In C_3 plants at 25°C and current atmospheric [CO_2], photorespiration results in an approximately 30% decrease in net carbon assimilation (Zhu et al., 2010). Thus, it is a large inefficiency in carbon uptake and a target for improvement.

Since CO_2 and oxygen act competitively at Rubisco, photorespiration can be decreased by increasing [CO_2] around Rubisco. That this will increase yield is demonstrated by the many studies that have artificially increased atmospheric [CO_2] around C_3 crops growing in the field (Kimball et al., 2002; Long et al., 2006b). Other photosynthetic organisms have evolved mechanisms to internally elevate [CO_2] at Rubisco to decrease or eliminate photorespiration. Such carbon-concentrating mechanisms (CCMs) include C_4 photosynthesis, as in maize (*Zea mays*), and the carboxysome and pyrenoid CCMs of single-celled cyanobacteria and algae. The C_4 pathway requires the addition of the photosynthetic C_4 dicarboxylate cycle and inner photosynthetic cells (i.e. bundle sheath), where Rubisco is localized. Converting a C_3 crop to a C_4 crop will require a coordination of changes in photosynthetic tissue differentiation and enzyme and transporter localization. In contrast, cyanobacteria achieve the same effect in a single cell by localizing Rubisco to specialized subcellular compartments called carboxysomes, so in theory they would require fewer changes. Carboxysomes are polyhedral bodies with a protein shell that encloses carbonic anhydrase (CA) and Rubisco packed in an ordered or semiordered array (Long et al., 2007; Yeates et al., 2011). Bicarbonate is actively transported from the environment into the cytosol of the cyanobacteria, and CO_2 in

[1] This work was supported by the National Science Foundation (grant no. EF–1105584) and the Bill and Melinda Gates Foundation.

* Address correspondence to slong@illinois.edu.

The author responsible for distribution of materials integral to the findings presented in this article in accordance with the policy described in the Instructions for Authors (www.plantphysiol.org) is: Stephen P. Long (slong@illinois.edu).

[W] The online version of this article contains Web-only data.

[OPEN] Articles can be viewed online without a subscription.

www.plantphysiol.org/cgi/doi/10.1104/pp.113.232611

the cytosol is actively hydrated to HCO_3^- using NADH. CO_2 is also hydrated to HCO_3^-, which serves to increase the [CO_2] gradient between the medium and cytosol, increasing CO_2 flux, and also serves to refix CO_2 that leaks from the carboxysome. Since the cytosol lacks CA and the plasma membrane has low permeability to HCO_3^-, a high cytosolic [HCO_3^-] far from equilibrium with [CO_2] is achieved. Bicarbonate diffuses through the protein shell of the carboxysome, and since CA is localized to the inner side of the shell, it is rapidly converted to CO_2, given the disequilibrium. The resulting high [CO_2] around Rubisco inside the carboxysome accelerates carboxylation and competitively inhibits the oxygenation reaction (for review, see Price et al., 2008, 2011, 2013; Espie and Kimber, 2011).

The C_4 pathway has been well characterized, and several projects are attempting to engineer it into C_3 plants with some success (Slewinski, 2013). However, a primary obstacle has been achieving the necessary two tissue types with the correct localization of the key enzymes (Covshoff and Hibberd, 2012). In this regard, cyanobacterial CCM may provide an attractive parallel approach to eliminating photorespiration in C_3 plants for two reasons. First, the biochemical, structural, and genetic components of the CCM are well understood, in that all of the necessary proteins and their genes have been identified. Second, chloroplasts of higher plants evolved from a common ancestor with modern cyanobacteria (Raven and Allen, 2003) and, therefore, are structurally similar. Thus, engineering carboxysomes into the chloroplast could involve introducing an operon containing the genes associated with the cyanobacterial CCM into the chloroplast genome.

There are, however, multiple proteins in the cyanobacterial CCM, and simultaneously transforming all of the required genes into an organism may be particularly challenging. Furthermore, some of the proteins appear to have a similar function, and others may be deleterious if introduced without the full apparatus. A random sequence of gene stacking would likely be inefficient, while the addition of some genes may simply be unnecessary. However, the biophysical reactions involved are well understood, and there are some measurements of the kinetics of the enzymatic reactions and transporters. With this information, a mathematical model can be created to simulate the CCM. Such a model will allow deduction of the minimal component set necessary for an improvement of leaf photosynthetic efficiency and identify a logical sequence of gene additions to deliver progressive improvements and avoid any lethal effects. This model will also be used to determine which aspects of the CCM exert the most control over the overall process of photosynthetic CO_2 assimilation, information that can then be used to optimize the CCM, help identify the ideal set of components, or identify parameters that need to be more accurately measured in order to improve the effectiveness of the CCM model. Similar kinetic models have been applied to propose systems optimization of the Calvin cycle when plants are grown in elevated [CO_2] (Zhu et al., 2007), of the whole C_3 photosynthetic system (Zhu et al., 2013), C_4 photosynthesis (Yu et al., 2014), and to determine the mechanistic basis of mesophyll conductance (Tholen and Zhu, 2011).

This paper develops a kinetic model to determine the potential of the cyanobacterial CCM engineered into C_3 crops for improving photosynthesis by determining the necessary components and estimating the potential improvement of CO_2 assimilation rate and efficiency. There are four distinct features to the cyanobacterial CCM: (1) a carboxysome with internally localized Rubisco and CA; (2) active transport of HCO_3^- from the medium into the cyanobacterial cytosol (the equivalent compartment in higher plants is the stroma of the chloroplast); (3) active hydration of CO_2 to HCO_3^- within the cytosol; and (4) the absence of CA in the cyanobacterial cytosol, in contrast to the higher plant stroma, which contains high activities of CA. Cyanobacteria have three HCO_3^- transporters and two CO_2 hydration enzymes that have different kinetics and are induced under different conditions (Price et al., 2011). All of these enzymes were examined, giving a total of seven individual components (listed in Fig. 1A) to the full cyanobacterial CCM model. Because of the common ancestry between cyanobacteria and higher plant chloroplasts, the two have homologous membranes and compartments. Proteins were modeled within a C_3 leaf using locations equivalent to those in cyanobacteria. That is, bicarbonate transporters were localized to the inner chloroplast membrane, and carboxysomes were localized to the stroma. The CO_2 hydration enzymes are bound to the thylakoid and plasma membranes in cyanobacteria, but the reaction for both occurs within the cyanobacterial cytosol; therefore, in this model, hydration of CO_2 by these enzymes was localized to the stroma. This model was used to determine the necessity of each of the features noted above, potential improvements in light-saturated CO_2 uptake (A_{sat}; irradiance of 1,800 μmol photons m^{-2} s^{-1}) that would be achieved on incorporation of each feature in turn, a possible sequence of gene additions that would give an incremental improvement, and the key components of the CCM. The model was also used to test the value of using higher plant isoforms of Rubisco versus prokaryotic isoforms adapted to incorporation within the carboxysome. Sources of uncertainty in the model are also defined.

RESULTS

Incorporating the four key features (composed of seven individual components) of a cyanobacterial CCM into a C_3 leaf increased A_{sat} from 23.8 to 38 μmol m^{-2} s^{-1} in this model (Fig. 1). The majority of changes that involved the addition of only a single feature decreased A_{sat}, sometimes to levels that would greatly reduce plant growth and probably require rescue in high [CO_2] (a list of all possible combinations of features

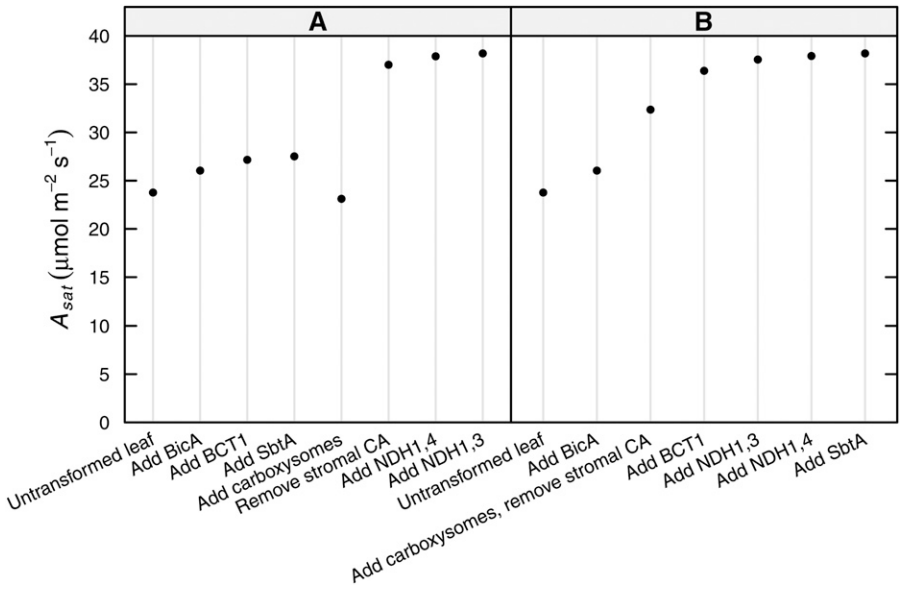

Figure 1. A_{sat} of leaf models with sequential addition of components of the cyanobacterial CCM. Each point represents a leaf that contains the component listed for that column and all of the components in the columns to the left of it. The columns represent the sequence of transformations that produce the fastest increase in A_{sat} assuming that it is not possible to simultaneously add carboxysomes and remove stromal CA and that it is not desirable to add CO_2 hydration enzymes before removal of stromal CA (A) and assuming that it is possible to simultaneously add carboxysomes and remove stromal CA (B).

and their effects on A_{sat} is given in Supplemental Table S1). However, addition of any one of the HCO_3^- transporters, bicarbonate uptake A (BicA), bicarbonate transporter1 (BCT1), or sodium-bicarbonate transporter A (SbtA) alone, improved A_{sat}. The addition of carboxysomes without removal of stromal CA or vice versa was detrimental to A_{sat} regardless of the inclusion of other features. Thus, unless it is possible to simultaneously add carboxysomes and remove stromal CA, there is no series of transformations that provides increased A_{sat} at each stage. Without the ability to make those changes simultaneously, the results here indicate that the best pathway of improvement is to first add the HCO_3^- transporters, add carboxysomes, remove stromal CA, and then add the NADH-driven CO_2 hydration enzymes (Fig. 1A). If it is possible to add carboxysomes and remove stromal CA simultaneously, then a slightly different pathway provides faster initial improvement, as follows: adding (1) BicA, (2) carboxysomes with simultaneous removal of CA, (3) BCT1, (4) NAD(P)H dehydrogenase complex (NDH1,3), (5) NDH1,4, and (6) SbtA (Fig. 1B). The final result is the same regardless of which sequence of transformations is used (last columns in Fig. 1).

At minimum, in order for the carboxysome to be effective requires the removal of stromal CA and the addition of BicA, BCT1, or NDH1,3 (Supplemental Table S1). Individually, neither SbtA nor NDH1,4 increase the stromal [HCO_3^-] enough for the carboxysome to be effective. Although at the enzyme concentrations modeled, the HCO_3^- transporters are more effective than CO_2 hydration enzymes at increasing A_{sat}, since the CO_2 hydration and HCO_3^- transport enzymes use different forms of energy, it may be desirable to include one of each type of enzyme so that the system is more flexible. If only one HCO_3^- transporter and one NDH isoform can be incorporated with a carboxysome, the pair that gives the highest A_{sat} is BicA with NDH1,3 (Supplemental Table S1).

In the absence of a CCM, replacement of the C_3 crop Rubisco with a cyanobacterial or algal isoform of Rubisco resulted in a 5% to 50% decrease in A_{sat} (Fig. 2). However, when the addition of the CCM is simulated and Rubisco is assumed to be confined to the carboxysome, this disadvantage is eliminated for most of the cyanobacterial, bacterial, and algal isoforms, where, in the high [CO_2] of the carboxysome, rates were often similar to, but did not exceed, those of the higher plant isoforms (Fig. 2).

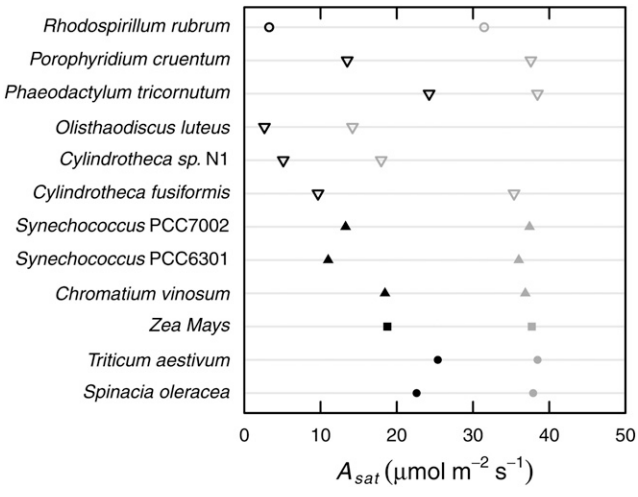

Figure 2. A_{sat} of leaf models without (black symbols) and with (gray symbols) a cyanobacterial CCM using different isoforms of Rubisco. Species from which the Rubisco isoform parameters were used are listed on the vertical axis. Parameters for the isoforms are given in Supplemental Table S2. Symbols represent the class of species: closed circles, C_3; closed squares, C_4; closed triangles, cyanobacteria; open triangles, nongreen algae form I; and open circles, nongreen algae form II (where form I and form II are as defined by Gibson and Tabita [1977]).

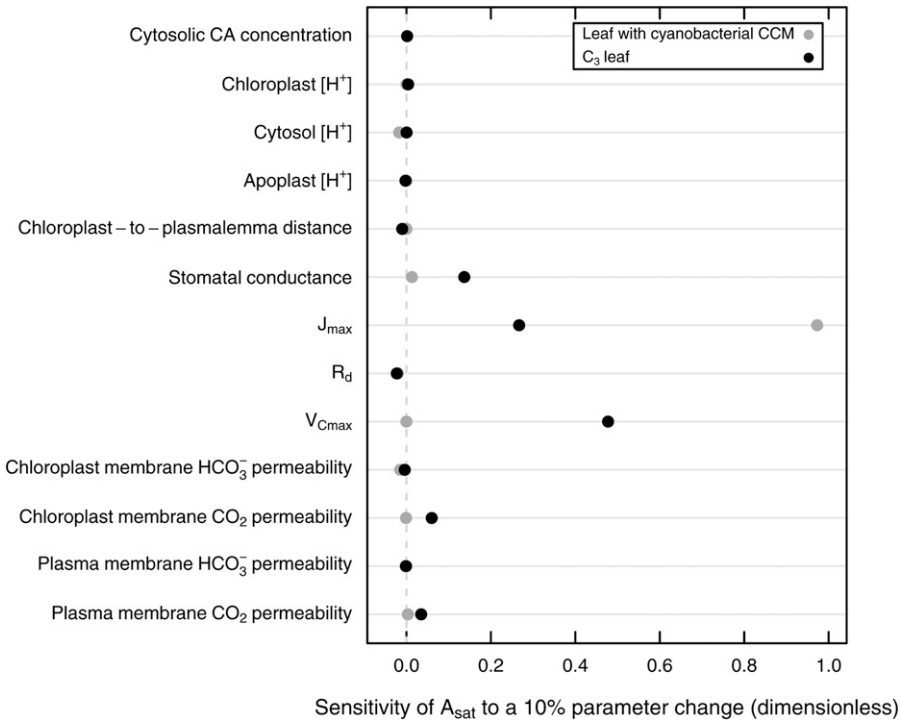

Figure 3. Sensitivity of the predicted A_{sat} to model parameters for leaf C_3 photosynthesis without (black circles) or with (gray circles) the addition of the cyanobacterial CCM. R_d, Mitochondrial respiration in the light.

In order to determine how limitations to photosynthesis are changed in a leaf with a CCM, the sensitivity of A_{sat} to several parameters in the model was compared between an untransformed leaf and a leaf with all seven of the changes listed in Figure 1A. In the transformed leaf, A_{sat} was very sensitive to the maximum rate of electron transport (J_{max}), with slight sensitivity to stomatal conductance and cytosolic [H^+] (Fig. 3). Following Farquhar et al. (1980), we use the term J_{max}. During the development of that model, it was

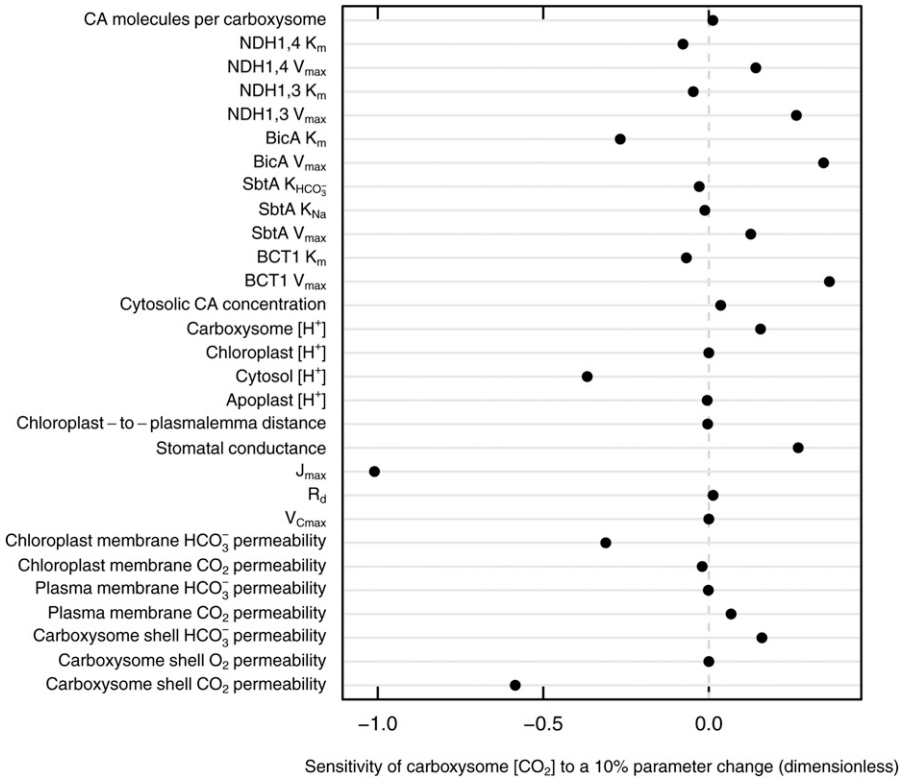

Figure 4. Sensitivity of carboxysomal [CO_2] to variation in model parameters for leaf C_3 photosynthesis with the simulated addition of the cyanobacterial CCM. R_d, Mitochondrial respiration in the light.

Table I. *Parameters, values, and their sources*

Name	Symbol	Value	Units	References
Temperature	T	298.15	K	25°C
Pressure	*pressure*	101,325	Pa	Atmospheric pressure
Gas constant	R	8.31446	J mol^{-1} K^{-1}	Universal gas constant
Atmospheric [CO_2]	C_a	390×10^{-6}	mol mol^{-1}	Approximate atmospheric [CO_2] in 2012
Oxygen partial pressure	O	*pressure* × 0.208	Pa	21% oxygen
Solubility of CO_2	$H_{CO_2}H_{CO2}$	2,994.012	m^3 Pa^{-1} mol^{-1}	von Caemmerer (2000)
Solubility of oxygen	H_{O_2}	79,365.1	m^3 Pa^{-1} mol^{-1}	von Caemmerer (2000)
CO_2 diffusivity in water	D_{CO_2,H_2O}	1.7×10^{-9}	m^2 s^{-1}	Terashima et al. (2011)
HCO_3^- diffusivity in water	$D_{HCO_3^-,H_2O}$	$D_{CO_2,H_2O} \times 0.56$	m^2 s^{-1}	Evans et al. (2009)
Molarity of air	n_{air}	40.87	mol m^{-3}	Calculated from T, R, and *pressure* using the ideal gas law.
Boundary thickness	l_b	0.0005	m	Nobel (1983); 10-cm leaf at about 1 m s^{-1} wind speed
Cell wall thickness	l_w	0.32×10^{-6}	m	Pritchard et al. (1986)
Chloroplast-to-plasmalemma distance	$l_{thin\ cytosol}$	0.1×10^{-6}	m	Evans et al. (2009)
Boundary layer conductance	g_b	1.53	mol m^{-2} s^{-1}	Calculated from l_b
Stomatal conductance	g_s	0.4375	mol m^{-2} s^{-1}	Bernacchi et al. (2006)
Mesophyll surface area fraction	S_m	15	m^2 m^{-2} (exposed mesophyll surface area per one-sided leaf area)	Slaton and Smith (2002)
Carboxysome surface area fraction	S_{csome}	72.75	m^2 m^{-2} (surface area per one-sided leaf area)	Long et al. (2007)[a]
CO_2 transfer coefficient	k_{tr}	$\frac{D_{CO_2,H_2O}}{l_w/10}$	m s^{-1}	Assumed that CO_2 dissolution into the cell wall only occurs in the one-tenth of the wall adjacent to the airspace
Cell wall porosity	ϕ_{apo}	0.2	Dimensionless	Evans et al. (2009)
Cell wall tortuosity	τ_{apo}	1	Dimensionless	Evans et al. (2009)
Plasmalemma permeability to CO_2	P_{p,CO_2}	0.0035	m s^{-1}	Gutknecht et al. (1977)
Plasmalemma permeability to HCO_3^-	P_{p,HCO_3^-}	0.5×10^{-6}	m s^{-1}	Tholen and Zhu (2011)
Chloroplast envelope permeability to CO_2	P_{chl,CO_2}	$P_{p,CO_2}/2$	m s^{-1}	Calculated using two membrane layers of the envelope
Chloroplast envelope permeability to HCO_3^-	P_{chl,HCO_3^-}	$P_{p,HCO_3^-}/2$	m s^{-1}	Calculated using two membrane layers of the envelope
Mitochondrial membrane permeability to CO_2	P_{m,CO_2}	$P_{p,CO_2}/2$	m s^{-1}	Calculated using two membrane layers of the mitochondrion
Mitochondrial membrane permeability to HCO_3^-	P_{m,HCO_3^-}	$P_{p,HCO_3^-}/2$	m s^{-1}	Calculated using two membrane layers of the mitochondrion
Carboxysome shell permeability to CO_2	P_{csome,CO_2}	$D_{glut,O_2}/l_{shell}$	m s^{-1}	Assumed
Carboxysome shell permeability to oxygen	P_{csome,O_2}	$D_{glut,O_2}/l_{shell}$	m s^{-1}	Assumed
Carboxysome shell permeability to HCO_3^-	P_{csome,HCO_3^-}	P_{p,CO_2}	m s^{-1}	Assumed
Gluten film oxygen diffusivity	D_{glut,O_2}	0.0914×10^{-12}	m^2 s^{-1}	Perez-gago and Krochta (2001)

(*Table continues on following page.*)

Table I. (*Continued from previous page.*)

Name	Symbol	Value	Units	References
Carboxysome shell thickness	l_{shell}	0.03×10^{-6}	m	Long et al. (2007)
Chloroplast surface area fraction	S_{chl}	0.75	$m^2\ m^{-2}$ (surface area appressed to the plasmalemma per mesophyll surface area)	Tomás et al. (2013)
Mitochondria surface area fraction	S_{mito}	0.12	$m^2\ m^{-2}$ (surface area appressed to the plasmalemma per mesophyll surface area)	Tholen and Zhu (2011)
Cytosol viscosity	$v_{cytosol}$	2	Dimensionless (relative to water)	Tholen and Zhu (2011); compare with Scalettar et al. (1991) and Köhler et al. (2000)
Stroma viscosity	v_{stroma}	10	Dimensionless (relative to water)	Tholen and Zhu (2011); compare with Köhler et al. (2000)
Carboxysome viscosity	v_{csome}	v_{stroma}	Dimensionless (relative to water)	Assumed
CA k_{eq} ($[HCO_3^-] \times [H^+]/[CO_2]$)	k_{eq}	0.56×10^{-6}	$mol\ m^{-3}$	Pocker and Miksch (1978)
CA k_{cat}	$k_{h,cat}$	0.3×10^{6}	s^{-1}	Larsson et al. (1997)
CA $K_{m,CO2}$	$K_{h,c}$	1.5	$mol\ m^{-3}$	Pocker and Ng (1973)
CA $K_{m,HCO3}$	$K_{h,b}$	34	$mol\ m^{-3}$	Pocker and Miksch (1978)
Rubisco maximum rate of carboxylation	$V_{c,max}$	7.6	$mol\ m^{-3}\ s^{-1}$	Bernacchi et al. (2005)[b]
Rubisco carboxylation rate constant	$k_{c,cat}$	2.87	$site^{-1}\ s^{-1}$	von Caemmerer (2000)
Rubisco Michaelis-Menten constant for CO_2	K_c	0.0086	$mol\ m^{-3}$	von Caemmerer (2000)[c]
Rubisco Michaelis-Menten constant for oxygen	K_o	0.215	$mol\ m^{-3}$	von Caemmerer (2000)[c]
CO_2 photocompensation point	Γ^*	1.29×10^{3}	$mol\ m^{-3}$	von Caemmerer (2000)[c]
Maximum rate of RuBP regeneration	J_{max}	13.7	$mol\ m^{-3}\ s^{-1}$	Bernacchi et al. (2002) at 25°C[b,d]
SbtA Michaelis-Menten constant for Na	K_{Na}	1.048	$mol\ m^{-3}$	Shibata et al. (2002)[e]
SbtA Michaelis-Menten constant for HCO_3^-	$K_{HCO_3^-}$	0.019	$mol\ m^{-3}$	Shibata et al. (2002)[e]
SbtA maximum rate of HCO_3^- transport	$V_{max,sbta}$	22.48×10^{-6}	$mol\ m^{-2}\ s^{-1}$	Shibata et al. (2002)[e,f]
BicA Michaelis-Menten constant for HCO_3^-	$K_{m,bica}$	0.217	$mol\ m^{-3}$	Price et al. (2004)
BicA maximum rate of HCO_3^- transport	$V_{max,bica}$	185×10^{-6}	$mol\ m^{-2}\ s^{-1}$	Price et al. (2004)[f]
BCT1 Michaelis-Menten constant for HCO_3^-	$K_{m,bct1}$	0.015	$mol\ m^{-3}$	Omata et al. (2002)
BCT1 maximum rate of HCO_3^- transport	$V_{max,bct1}$	55×10^{-6}	$mol\ m^{-2}\ s^{-1}$	Omata et al. (1999)[f]
NDH1,3 Michaelis-Menten constant for CO_2	$K_{m,ndh13}$	0.012	$mol\ m^{-3}$	Price et al. (2011)
NDH1,3 maximum rate of CO_2 hydration	$V_{max,ndh13}$	0.075	$mol\ m^{-2}\ s^{-1}$	Berner (1993)[g]; David et al. (2002)

(*Table continues on following page.*)

Table I. (*Continued from previous page.*)

Name	Symbol	Value	Units	References
NDH1,4 Michaelis-Menten constant for CO_2	$K_{m,ndh14}$	0.002	mol m^{-3}	Price et al. (2011)
NDH1,4 maximum rate of CO_2 hydration	$V_{max,ndh14}$	$V_{max,ndh13}$	mol m^{-2} s^{-1}	Berner (1993)[g]; David et al. (2002)
Mitochondrial respiration in the light	R_d	1.98	mol m^{-3} s^{-1}	Bernacchi et al. (2002) at 25°C
Stromal CA concentration	$[CA]_{stroma}$	0.27	mol m^{-3}	Tholen and Zhu (2011); compare with Gillon and Yakir (2000)
Mitochondrial CA concentration	$[CA]_{mito}$	$[CA]_{stroma}$	mol m^{-3}	Assumed
Cytosolic CA concentration	$[CA]_{cyto}$	$[CA]_{stroma}/2$	mol m^{-3}	Tholen and Zhu (2011)
Apoplastic CA concentration	$[CA]_{apo}$	$[CA]_{stroma}/2$	mol m^{-3}	Assumed
Stroma mesophyll volume fraction	f_{stroma}	0.147	m^3 m^{-3} (volume per mesophyll cell volume)	Winter et al. (1994)
Cytosol mesophyll volume fraction	$f_{cytosol}$	0.054	m^3 m^{-3} (volume per mesophyll cell volume)	Winter et al. (1994)
Airspace volume fraction	None	0.5	m^3 m^{-3} (volume per bulk volume of leaf)	Byott (1976)
Stroma volume fraction	None	0.87×10^{-6}	m^3 m^{-2} (volume per mesophyll surface area)	Tholen and Zhu (2011)
Mitochondria volume fraction	None	0.027×10^{-6}	m^3 m^{-2} (volume per mesophyll surface area)	Tholen and Zhu (2011)
Leaf chlorophyll	None	0.5	g m^{-2}	Daughtry et al. (2000)

[a]The number of carboxysomes was chosen so that the concentration of Rubisco as mol m^{-2} was the same as a leaf without carboxysomes. [b]Converted to a volumetric basis from a leaf-area basis using values of 100 and 180 μmol m^{-2} s^{-1} for $V_{c,max}$ and J_{max}. [c]Calculated from Table 1.3 of von Caemmerer (2000) using solubilities of 0.0034 and 0.00126 mol L^{-1} bar^{-1} for CO_2 and oxygen, respectively. [d]When the model of Farquhar et al. (1980) was developed, the rate of RuBP regeneration was assumed to be entirely limited by the rate of electron transport. Thus, the symbol J_{max} was used. It is now known that processes other than electron transport can limit RuBP regeneration. Here, we use the same symbol for continuity, but with the understanding that it represents RuBP regeneration, potentially being limited by several factors. [e]Values were determined from Shibata et al. (2002) by fitting data to a two-substrate sequential enzyme reaction model. [f]Assuming the same amount of protein per chlorophyll in cyanobacteria and leaf chlorophyll concentration from Daughtry et al. (2000). [g]Values for protein concentration in cyanobacteria for these enzymes were obtained through personal communication with G. Dean Price. Values were calculated assuming that higher plants would have the same protein concentration per area of thylakoid membrane as in cyanobacteria. There were multiple estimates of V_{max} and thylakoid surface area. To represent a typical value, the mean of the highest and lowest estimates was used.

assumed that RuBP regeneration was limited solely by electron transport, but it is now known that enzyme activity in the Calvin cycle also limits RuBP regeneration (Lefebvre et al., 2005). Thus, when we refer to J (for rate of RuBP regeneration) and J_{max}, this actually represents RuBP regeneration with the understanding that it may be limited by Calvin cycle activity or electron transport rate. Because assimilation is saturated at high $[CO_2]$, A_{sat} in the transformed leaf will be insensitive to the many factors that limit CO_2 transfer and $[CO_2]$ at Rubisco in the untransformed leaf. Therefore, the sensitivity of $[CO_2]$ within the carboxysome was also determined to assess which parameters most influence the CCM (Fig. 4). In this case, the carboxysomal $[CO_2]$ in the transformed leaf was similarly most sensitive to J_{max}, but several other parameters exerted strong influence, in particular the carboxysome shell permeability to CO_2 and HCO_3^-, the carboxysomal and cytosolic pH, the K_m of BicA, and the V_{max} of BicA, BCT1, and NDH1,3 (Fig. 4).

To determine how the permeability of the protein shell to CO_2 affects the effectiveness of the CCM, the coefficient of permeability was varied across a range of plausible values. Although low permeability to CO_2 is a key characteristic of the protein shell (Dou et al., 2008; Cai et al., 2009), the actual permeability to CO_2 has never been quantitatively measured directly or indirectly, and in this model it could only be assumed that is was similar to thin films of other proteins, in this case, whey protein isolate (Perez-gago and Krochta, 2001). Since there is such uncertainty in this parameter, it is desirable to know whether it could realistically have a value at which the cyanobacterial CCM would not be effective if introduced into a C_3 leaf. The lower limit is zero permeability, and a reasonable upper limit is the same permeability to CO_2 as lipid bilayer membranes, which are relatively permeable to small, uncharged molecules such as CO_2 compared with protein layers ($P_{p,CO2}$ compared with $P_{csome,CO2}$ in Table I). A modeled

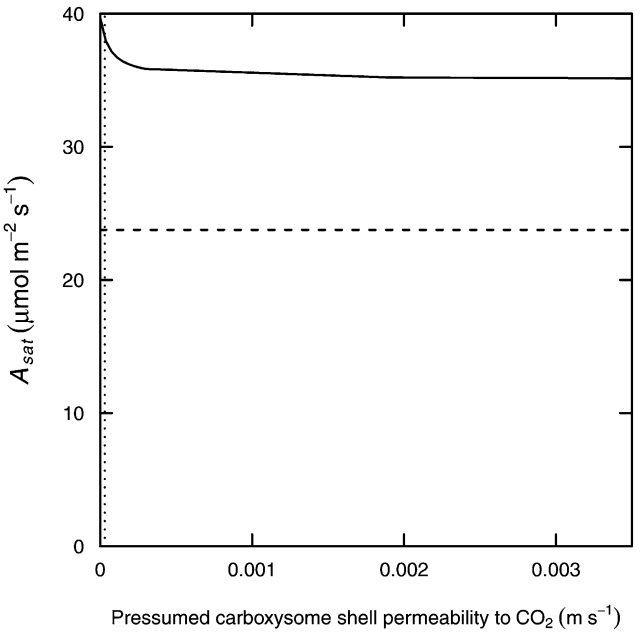

Figure 5. Predicted A_{sat} for a C_3 leaf with the simulated addition of the cyanobacterial CCM plotted against varying assumed permeabilities of the carboxysome protein shell to CO_2. The range of permeabilities was chosen so that it would encompass all plausible values. The lower limit is zero permeability, and a reasonable upper limit is the same permeability to CO_2 as lipid bilayer membranes, which are quite permeable to small, uncharged molecules such as CO_2. The vertical dotted line is the best estimate for permeability, which was used in all other predictions (Figs. 1–5 and 7). The horizontal dashed line is the modeled assimilation rate of a C_3 leaf without a CCM.

leaf with a CCM had higher values of A_{sat} compared with a modeled leaf without a CCM regardless of the assumed permeability of the shell to CO_2 (Fig. 5). The CCM becomes more effective as shell CO_2 permeability decreases, while A_{sat} shows high sensitivity to CO_2 permeability around the best estimate value for this parameter (Fig. 5).

Even though A_{sat} is not improved by using a cyanobacterial Rubisco isoform due to RuBP-regeneration limitation, carboxysomal [CO_2] is nearly high enough to take advantage of the higher k_{cat} of that isoform if the RuBP regeneration rate can be increased (Fig. 6). In saturating light, a modeled leaf with a cyanobacterial CCM was more efficient than a modeled C_3 leaf in terms of ATP use per net CO_2 fixation by Rubisco at internal airspace [CO_2] (C_i) below about 300 μmol mol^{-1} (Fig. 7), whereas in light-limited conditions, the CCM was more ATP efficient at C_i below about 150 μmol mol^{-1} (Fig. 7).

DISCUSSION

Potential Improvement to A_{sat}

The increase in A_{sat} from 23.8 to 38 μmol m^{-2} s^{-1} shown here from theory due to engineering a cyanobacterial CCM into C_3 species could have remarkable benefits for crop production, including increased yield, nitrogen use efficiency, and water use efficiency. Increasing leaf photosynthesis by 25% through artificial elevation of [CO_2] under open-air conditions in the field increased the yield of soybean (*Glycine max*) by 15% and water use efficiency by 20% to 40% (Long et al., 2006b; Bernacchi et al., 2007). In our simulation here, the 60% increase in A_{sat} that is predicted would by analogy allow a 36% increase in yield. The smaller increase in yield than in photosynthesis for crops grown in the field under elevated [CO_2] is suggested to result from sink limitation (i.e. the ability of the crop to make full use of the available additional photoassimilate; Ainsworth et al., 2004; Long et al., 2006a). Identifying germplasm with sufficient capacity to form grain or seed is considered less challenging than the generation of more resource to fill those grains or seed (Sheehy et al., 2001). Therefore, it might be expected that provision of an increase in photosynthetic efficiency of 60% could, with some breeding, be matched by an equal yield increase.

The prediction here is for A_{sat} (i.e. light-saturated photosynthesis). Typically, about half of crop carbon gain is from light-limited photosynthesis (Baker et al., 1988). Here, though, an increase in photosynthesis would also be expected, since the maximum efficiency of carbon assimilation under light-limiting conditions is determined by the ratio of carboxylations to oxygenations at Rubisco. The model results indicate that the CCM was more ATP use efficient in light-limited conditions for C_i below about 150 μmol mol^{-1} (Fig. 7). The difference between light conditions occurs because in RuBP regeneration-limited photosynthesis, CO_2 uptake saturates at a lower C_i than HCO_3^- transport. Therefore, as C_i increases, HCO_3^- transport increases more than CO_2 uptake and ATP/CO_2 increases. In low light, photosynthesis is limited by RuBP regeneration at a lower C_i, making this effect apparent at approximately 50 μmol mol^{-1} CO_2 (Fig. 7). Although initially this suggests that the CCM is not as beneficial in light-limited conditions, if HCO_3^- transport were regulated to be proportional to light levels or inversely proportional to stromal [HCO_3^-], the efficiency in light-limited conditions would be higher than presented here. Regulation of these transporters has not been thoroughly studied, but some are inducible (Price et al., 2013), and it is reasonable to assume that they are disabled in the dark in the cyanobacterial system or that there would be futile cycling of CO_2 in the dark. That suggests that their activity could also be proportional to light intensity. Therefore, the concentration of CO_2 at Rubisco would be expected to increase not just light-saturated photosynthesis but also canopy photosynthesis to a similar degree.

Cyanobacterial and algal Rubisco isoforms performed very poorly under conditions assumed to operate in the normal C_3 plastid (i.e. without a CCM; Fig. 2). This is to be expected, given that they presumably reflect millions of years of evolution to operate in a high [CO_2] environment, with their low specificity resulting in high oxygenation rates in the

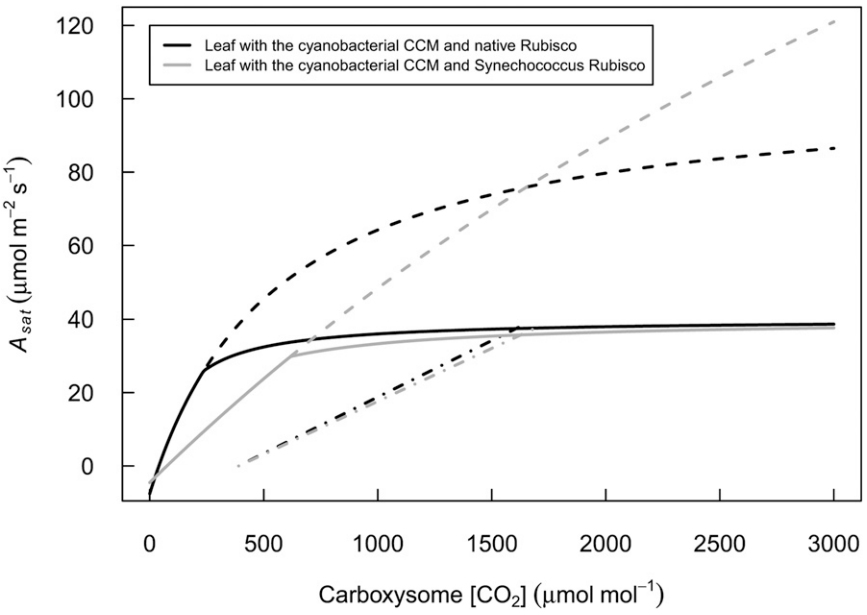

Figure 6. Predicted A_{sat} versus carboxysome [CO_2] for C_3 (black lines) and cyanobacterial (gray lines) isoforms of Rubisco. Solid lines are modeled A_{sat}. Dashed lines are the net carboxylation rate of Rubisco if RuBP regeneration were not limiting. Dotted-dashed lines are the supply function from the atmosphere to the carboxysome. The [CO_2] at the *x* intercept is atmospheric [CO_2], where the supply function intercept assimilation rate is the [CO_2] in the carboxysome and A_{sat} in atmospheric [CO_2] (390 μmol mol^{-1}).

low [CO_2] of the C_3 leaf chloroplast. Although the performance of these isoforms of Rubisco was increased greatly by the addition of the cyanobacterial CCM, none of these isoforms substantially outperformed the higher plant isoforms, despite their higher turnover number (k_{cat}) per active site. This resulted because in the modeled system, the rate of RuBP regeneration and not the rate of carboxylation was limiting, preventing a stronger response in A_{sat} and explaining the high sensitivity of the system to J (Figs. 3 and 4). Thus, at elevated [CO_2], most Rubisco isoforms support a similar A_{sat}, as simulated (Fig. 2). However, replacing the C_3 crop Rubisco with a cyanobacterial isoform could still be of value. First, cyanobacterial Rubisco can assemble in a lattice form, and the carboxysome shell can enclose this. It is not known whether this is possible with higher plant or any eukaryotic Rubisco, so introducing the cyanobacterial Rubisco along with the carboxysome shell structure into the chloroplast would remove this uncertainty. Second, model results show that this CCM is capable of increasing carboxysomal [CO_2] to levels high enough to take advantage of the higher k_{cat} of the cyanobacterial Rubisco isoform (Fig. 6), which could be utilized in two ways: increasing A_{sat} by increasing the capacity for RuBP regeneration or decreasing Rubisco concentration while maintaining the same A_{sat}. Recent theoretical and practical evidence suggests that reoptimization of investment within the Calvin cycle could increase the rate of RuBP regeneration (Lefebvre et al., 2005; Zhu et al., 2007). RuBP regeneration might also be increased by increasing the maximum rate of whole-chain electron transport, which is suggested to be limited by the amount of cytochrome b_6/f complex (Price et al., 1998; Ruuska et al., 2000). However, even with RuBP regeneration limiting photosynthesis, at high carboxysomal [CO_2], a Rubisco isoform with a high k_{cat} would allow for lower Rubisco concentrations than with a higher plant C_3 isoform but still maintain the same photosynthetic rate, improving nitrogen use efficiency (Long et al., 2004).

The cyanobacterial Rubisco isoforms saturate at much higher [CO_2] than C_3 isoforms ($K_{m,CO2}$ of 180 compared with 10 mmol m^{-3}; Fig. 6). The results here show that they are not saturated even at the simulated high [CO_2] of 1,700 μmol mol^{-1} achieved with the CCM here. Therefore, further increases in [CO_2] would still be beneficial. The sensitivity of carboxysomal [CO_2] to different system features indicates that the primary targets increase [CO_2] further. Here, parameters with sensitivity coefficients greater than 0.1 were considered important (i.e. a 1% change in the parameter resulted in a greater than 0.1% change in carboxysomal [CO_2]). Carboxysomal [CO_2] is sensitive to the V_{max} of BicA, BCT1, NDH1,3, and NDH1,4, suggesting that improving effectiveness may be as simple as increasing the activities of these enzymes (Fig. 4). In addition, the model is also sensitive to pH in both the carboxysome and cytosol (Fig. 4). The pH in the carboxysome will most likely be the same as in the stroma, since protons can readily cross the carboxysome shell (Menon, 2010), so altering carboxysomal pH would require changing stromal pH as well. However, it is not known how the diffusion of protons within the lattice of Rubisco will affect pH in the carboxysome. Since pH in both the cytosol and stroma is regulated, there are limits to altering pH in those compartments, but because sensitivity to these parameters is so high, even small changes should have a substantial effect. In addition to these factors, there are numerous anatomical features that are likely not optimized for a CCM, such as average cell volume, the exposed surface area of mesophyll

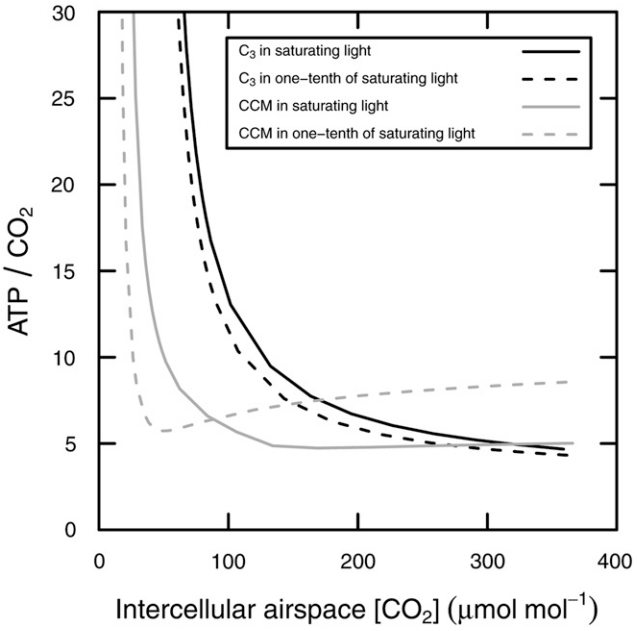

Figure 7. ATP use per net carboxylation by Rubisco ($v_{c,net} = v_c - v_o/2$) versus intercellular airspace [CO_2] in light-saturated (solid lines; 1,800 μmol photosynthetically active radiation m^{-2} s^{-1}) and light-limited (dashed lines; 180 μmol photosynthetically active radiation m^{-2} s^{-1}) conditions for a modeled C_3 leaf without (black lines) or with (gray lines) a cyanobacterial CCM.

cells, and cell wall thickness. Although altering these traits offers another route to improve the effectiveness of the CCM, examining all of them was beyond the scope of this study, whose primary aim was to assess the benefit of engineering the cyanobacterial CCM into the C_3 crop chloroplast.

Necessary Components and an Optimal Gene-Stacking Sequence

The CCM involves many components, some of which may prove more difficult to introduce than others. For example, two of the HCO_3^- pumps, BicA and SbtA, require single transformations targeted at the plastid envelope and should be relatively easy transformations (Burnell, 2011). The carboxysome shell, by contrast, is encoded by up to nine genes, one with multiple products, that must be expressed in correct proportions, and it requires the assembly of the shell around Rubisco and CA (Price et al., 1993; Ludwig et al., 2000; Long et al., 2007, 2010; Yeates et al., 2008; Kinney et al., 2011; Rae et al., 2012). It may also be difficult to attach effective transit peptides to each component, making plastid transformation a better option. However, plastid transformation has succeeded so far in only a few species and, as yet, in none of the major grain and seed crops (Maliga, 2004; Meyers et al., 2010). Of the four key features of the cyanobacterial CCM, the HCO_3^- transporters improve photosynthesis independently of other features (Fig. 1; Supplemental Table S1). In contrast, carboxysomes and removal of stromal CA are mutually dependent, and both have a strongly detrimental effect on simulated A_{sat} in the absence of the HCO_3^- transporters. This work suggests that while stacking all four major features of the cyanobacterial CCM would give by far the greatest benefit, an increase of 9% could be achieved by simply introducing the BicA transporter and an increase of 16% could be achieved by introducing BicA, BCT1, and SbtA together (Fig. 1A). This work also shows that this would be a valuable first step, since introducing the carboxysome and knocking out the stromal CA would be ineffective without HCO_3^- transporters. The total V_{max} for transport of HCO_3^- across the membrane is the sum of the V_{max} of each transporter. Thus, adding multiple transporters is more effective than adding a single transporter because it increases the V_{max} of total transport. In that respect, it could be equally as effective to simply express more of a single transporter than to introduce multiple transporters. However, the different affinities (Table I) suggest that the transporters allow for uptake at a wide range of [HCO_3^-], allowing the CCM to be effective across a wider range of C_i. This would be particularly useful if the inducibility of the transporters seen in cyanobacteria (Price et al., 2013) is preserved in the C_3 leaf, since that would allow for specific transporters to be inactivated at [HCO_3^-] where they are ineffective.

Key Model Parameters

The sensitivity of modeled C_3 and CCMs suggests that transformation of the complete cyanobacterial CCM into the chloroplast would result in the control of A_{sat} by stomatal conductance, the maximum rate of carboxylation by Rubisco ($V_{c,max}$), and the CO_2 permeabilities of the chloroplast envelope and plasma membranes would shift to J, which here refers to RuBP regeneration that can be limited by electron transport or the activity of enzymes in the Calvin cycle. As discussed earlier, increasing the amount of cytochrome b_6/f complex may be one approach to increase J_{max} (Price et al., 1998; Ruuska et al., 2000). Increasing J_{max} in C_3 species certainly seems possible, since C_4 species tend to have higher values of J_{max} than C_3 species (Wullschleger, 1993; Massad et al., 2007). There is also evidence that, in addition to electron transport, RuBP regeneration is colimited by enzyme activity in the Calvin cycle, specifically the amount of sedoheptulose-1,7-bisphosphatase (SBPase; Harrison et al., 2001), and increasing the concentration of SBPase has been shown to increase carbon assimilation and biomass in current atmospheric [CO_2] (Lefebvre et al., 2005). Moreover, the increase in biomass in an SBPase-overexpressing line compared with the wild type was larger in elevated [CO_2] compared with control [CO_2] (Rosenthal et al., 2011), which would be expected since in saturating light, rising [CO_2] shifts control from Rubisco to

the rate of RuBP regeneration (Long et al., 2004). This would make SBPase overexpression a target to add to a plant containing a successful cyanobacterial CCM.

Assessment of the sensitivity of predicted carboxysome [CO_2] to variation in parameters in the model (Fig. 4) had two purposes: (1) identifying the most effective components of the CCM and (2) identifying parameters in the model in most need of improved constraint, to focus effort to better understand the potential value of inclusion of the cyanobacterial CCM. The high sensitivity of the system to the kinetic properties of BicA and BCT1 underline the finding that the simulated inclusion of these HCO_3^- transporters alone will apparently increase A_{sat}, making them primary first targets for transformation. The complete CCM was also sensitive to the kinetic properties of the CO_2-hydrating enzyme NDH1,3, although this will depend on the diffusivity of CO_2 across the carboxysome shell. These enzymes serve the purpose of greatly steepening the CO_2 gradient between the atmosphere and stroma, thus accelerating CO_2 uptake into the chloroplast. In theory, the effect of this steepened gradient should be far more effective in the leaf than in a cyanobacterium, given that diffusivity is orders of magnitude greater in air than in water. There are few estimates of kinetic parameters for these transporters, though, so there is substantial uncertainty regarding their true kinetic properties and even amounts. This highlights a key need moving forward in assessing the real value of pursuing the addition of these proteins to crop plant plastids.

Equally, the system proved very sensitive to the assumed permeability of the protein shell (Figs. 4 and 5). The CCM is beneficial in terms of increasing A_{sat} across the plausible range of permeabilities (Fig. 5), indicating that, although there is little certainty in this value, the CCM provides a benefit regardless of the true permeability of the shell. Nonetheless, predictions of A_{sat} vary strongly depending on the value used and

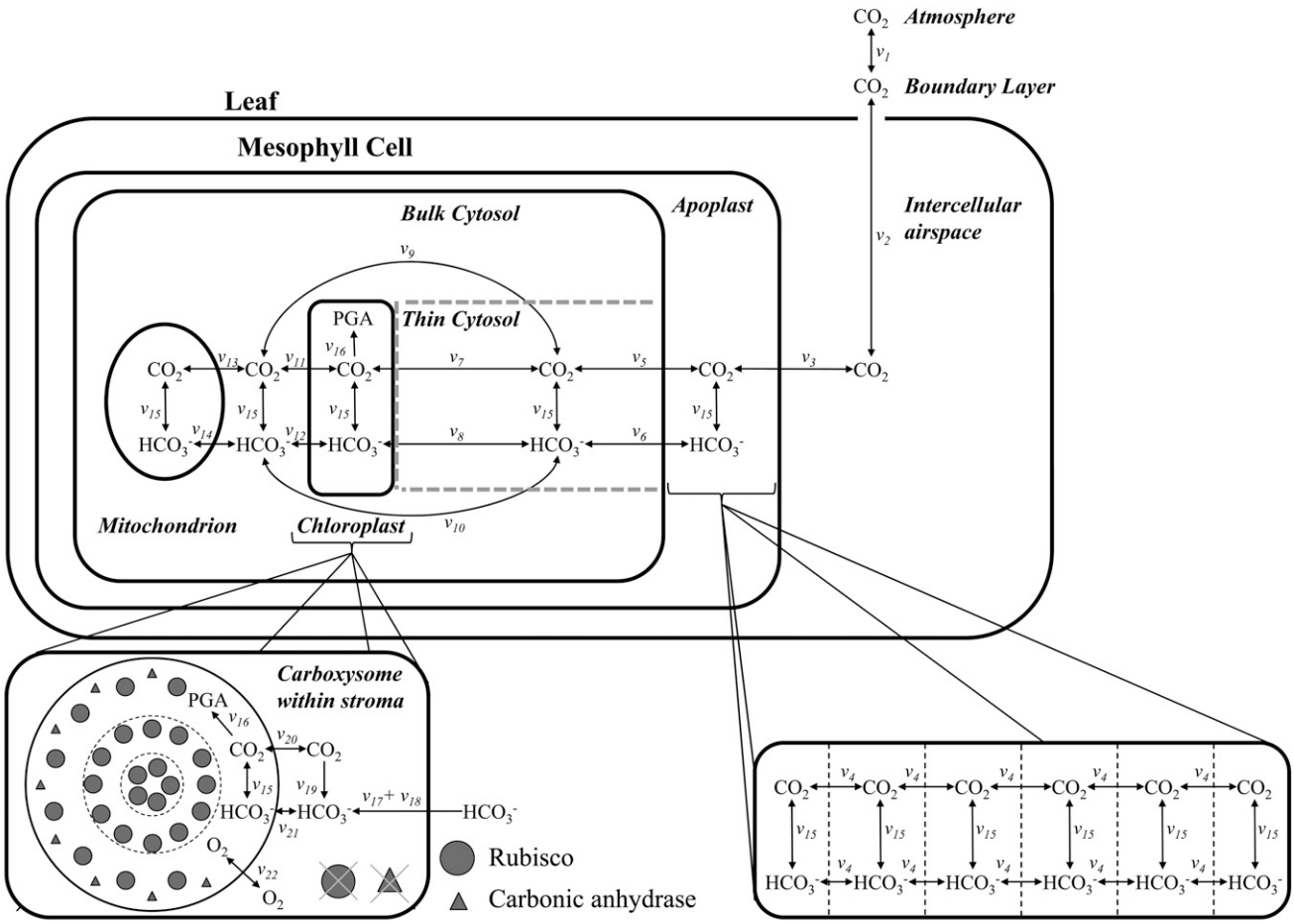

Figure 8. Compartments with the fluxes between pools in each compartment. The nine biological compartments of the model are labeled in boldface italic letters. The apoplast, thin cytosol, chloroplast stroma, and carboxysome compartments were each divided into size subcompartments to allow for nonlinear reactions of Rubisco and CA with their substrates. Pools are given in roman letters. Fluxes are labeled in italics, and rate equations for each flux are given in Supplemental Appendix S1.

are very sensitive to shell CO_2 permeability at the value used in this model (Figs. 4 and 5). Thus, better constraint of this parameter will be crucial to a more accurate quantification of the benefit of adding carboxysomes and the potential value of engineering the shell to decrease CO_2 permeability. The same argument can be made for the movement of HCO_3^- through the shell, particularly understanding whether this is a gated transfer (Klein et al., 2009). In contrast, the model is completely insensitive to permeability of the protein shell to oxygen. This is because oxygen in the atmosphere is very high at 21% and diffuses rapidly in air, so regardless of the permeability, large amounts of oxygen would diffuse into the carboxysome. Therefore, despite the fact that the true permeability to oxygen is also highly uncertain, obtaining better estimates will do little to improve the accuracy of model predictions.

CONCLUSION

This simulation of the addition of the cyanobacterial CCM to a C_3 crop leaf suggests that a nearly 60% improvement in net leaf CO_2 uptake could be achieved without any modification of leaf anatomy. By analogy to the artificial elevation of $[CO_2]$ in crop fields driving increased leaf CO_2 uptake, this could lead to a 36% to 60% increase in C_3 crop yield. The simulations suggest that the addition of the single BicA transporter would alone increase photosynthesis by 9% or 16% if all transporters are added. Beyond this, there is no benefit to introducing other components of the cyanobacterial CCM unless the complete CCM is added. Addition of carboxysomes and localization of Rubisco within this microcompartment would itself significantly depress leaf CO_2 uptake; their benefit is only achieved by minimally adding a plastid envelope HCO_3^- transporter such as BicA or a stromal CO_2 hydration enzyme such as NDH1,3 and complete removal of CA activity from the stroma. Introducing BicA and other transporters could be achieved by nuclear transformation and the inclusion of chloroplast envelope-targeting sequences. Achieving the full benefit of the cyanobacterial CCM will be considerably more challenging and most probably will depend on plastid transformation for expression of the shell proteins and an isoform of Rubisco adapted to packaging within the carboxysome.

MATERIALS AND METHODS

Carboxylation by Rubisco was simulated using the steady-state biochemical model of leaf photosynthesis of Farquhar et al. (1980):

$$v_c = \min\left(\frac{V_{c,max}\cdot[CO_2]}{[CO_2]+K_c\left(1+\frac{[O_2]}{K_o}\right)}, \frac{J\cdot[CO_2]}{4[CO_2]+8\Gamma^*}\right) \quad (1)$$

where v_c is the rate of carboxylation by Rubisco, $V_{c,max}$ (mol m^{-3} s^{-1}) and $[CO_2]$ (mol m^{-3}) are as defined above, $[O_2]$ (mol m^{-3}) is the oxygen concentration, K_c (mol m^{-3}) and K_o (mol m^{-3}) are the affinities of Rubisco for CO_2 and oxygen, J (mol m^{-3} s^{-1}) is as defined above, assumed to be limited by electron transport, and Γ^* (mol m^{-3}) is the CO_2 photocompensation point. Values for all parameters, and their sources, are given in Table I.

Oxygenation by Rubisco was calculated as by von Caemmerer (2000):

$$v_o = v_c\cdot\frac{2\cdot\Gamma^*}{[CO_2]} \quad (2)$$

where v_o is the rate of oxygenation by Rubisco. CO_2 was released in the mitochondria at a rate of $v_o/2$.

J was calculated as a function of the amount of light absorbed by PSII (I_2), J_{max}, and a curvature factor (θ), using a nonrectangular hyperbolic relationship of J to I_2:

$$J = \frac{I_2 + J_{max} - \sqrt{(I_2+J_{max})^2 - 4\theta\cdot I_2\cdot J_{max}}}{2\theta} \quad (3)$$

The amount of light absorbed by PSII (I_2) was calculated using an irradiance (I) of 1,800 μmol m^{-2} s^{-1}, leaf absorptance (α), and a light quality correction factor (f):

$$I_2 = I\cdot\frac{\alpha}{2}\cdot(1-f) \quad (4)$$

Reversible conversion between HCO_3^- and CO_2 by CA was modeled using Michaelis-Menten kinetics:

$$v_h = \frac{k_{h,cat}\cdot[CA]\cdot\left([CO_2]-\frac{[HCO_3^-]\cdot[H^+]}{K_{eq}}\right)}{K_{h,c}+\frac{K_{h,c}}{K_{h,b}}\cdot[HCO_3^-]+[CO_2]} \quad (5)$$

where $k_{h,cat}$ (s^{-1}) is the hydration rate constant, the concentrations ([CA], $[HCO_3^-]$, and $[H^+]$) are measured in mol m^{-3}, and $K_{h,c}$ (mol m^{-3}) and $K_{h,b}$ (mol m^{-3}) are the affinities of CA for CO_2 and HCO_3^-.

Bicarbonate transport across the chloroplast envelope by BCT1 and BicA was calculated using one-substrate Michaelis-Menten kinetics as:

$$v_t = \frac{V_{max}\cdot[HCO_3^-]}{[HCO_3^-]+K_m} \quad (6)$$

where V_{max} is the maximum rate of transport for BCT1 or BicA and K_m is the Michaelis-Menten constant of BCT1 or BicA for HCO_3^-.

Bicarbonate transport across the chloroplast envelope by SbtA was calculated using the two-substrate, sequential reaction Michaelis-Menten kinetics as from Alberty (1953):

$$v_t = \frac{V_{max}\cdot[Na]\cdot[HCO_3^-]}{[Na]\cdot[HCO_3^-]+K_{HCO_3^-}\cdot[Na]+K_{Na}\cdot[HCO_3^-]+K_{HCO_3^-}\cdot K_{Na}} \quad (7)$$

where V_{max} is the maximum rate of transport for SbtA and K_{HCO3-} and K_{Na} are the Michaelis-Menten constants for HCO_3^- and Na^+, respectively. Parameters for this enzyme were determined by fitting this model to data from Shibata et al. (2002).

Diffusion of CO_2 and HCO_3^- was modeled using various forms of Fick's law depending on the compartment. For diffusion across the boundary layer and intercellular space, a conductance was used:

$$\frac{dx}{dt} = g\cdot(x_1-x_2) \quad (8)$$

For diffusion across a membrane, a permeability was used:

$$\frac{dx}{dt} = P\cdot S\cdot(x_1-x_2) \quad (9)$$

And for diffusion within a gas or aqueous solution, a diffusivity was used:

$$\frac{dx}{dt} = \frac{D\cdot S}{v\cdot l}(x_1-x_2) \quad (10)$$

where x_1 and x_2 are concentrations of CO_2 or HCO_3^- in adjacent compartments, g (mol m^{-2} s^{-1}) is conductance of CO_2 across the stomata or boundary layer, P (m s^{-1}) is permeability of the membrane through which either CO_2 or HCO_3^- is diffusing, S (m^2) is the surface area of this membrane, D (m^2 s^{-1}) is diffusivity of HCO_3^- through liquid or CO_2 through liquid or air depending on the compartment, v (dimensionless) is the relative viscosity of the solution compared with water, and l (m) is the length of the diffusive path. Parameters were obtained by a literature search, and for anatomical characteristics, values for soybean (*Glycine max*) or similar species were used when available.

Diffusion was modeled from the atmosphere to the site of Rubisco via a potential nine compartments, as illustrated in Figure 8. The apoplast, thin cytosol, stroma, and carboxysome were each further divided into six subcompartments (for a total of 29 distinct compartments) in order to correctly estimate nonlinear reaction rates as described below. Since the majority of CO_2 in the cytosol diffuses via a short path to the chloroplast (Terashima et al., 2011), the cytosol was modeled as two compartments: the thin portion of cytosol (labeled "thin cytosol" in Fig. 8) between the plasmalemma and chloroplast envelope and the bulk cytosol comprising the rest of the cytosol.

For the model, the carboxysome was assumed to approximate a sphere, with a layer of CA on the immediate inside of the shell and then concentric layers of Rubisco filling the remainder of the space. The permeability of the protein shell to CO_2 and oxygen has not been determined quantitatively. In the absence of these measurements, it was assumed to be similar to a protein thin film, in this case whey protein isolate (Perez-gago and Krochta, 2001), corrected for the known thickness of the carboxysome protein shell (Long et al., 2007). Similarly, the permeability of the shell to HCO_3^- is unknown. Although HCO_3^- does not permeate lipid membranes easily, it is thought that the hexamers of the carboxysome shell form gated pores that allow selective permeation by HCO_3^- (Kerfeld et al., 2005; Klein et al., 2009). As a basis of comparison, it was reasoned that the shell should be as permeable to HCO_3^- as lipid membranes are to dissolved gases, so it was assumed that the permeability of the shell to HCO_3^- was similar to the permeability of CO_2 through a lipid bilayer. The consequence of uncertainty in these parameters was evaluated using a sensitivity analysis (Figs. 3–5). The number of carboxysomes was chosen so that they would contain the same number of Rubisco molecules in the C_3 leaf stroma, assuming 3,351 Rubisco molecules per carboxysome (Long et al., 2007), giving 2,700 carboxysomes per chloroplast. Carboxysomes are small compared with chloroplasts, and this number of carboxysomes accounts for only about 15% of the stromal volume.

Conversion between CO_2 and HCO_3^- via CA was modeled in all aqueous compartments except in model runs that explicitly remove CA. Since the reaction rates of CA and Rubisco are nonlinear with respect to substrate concentration, the mean concentration of substrate in the compartment cannot be used to calculate reaction rate, because substrate concentration decreases along the path of net diffusion. To allow for this nonlinear activity, the apoplast, chloroplast, thin cytosol, and carboxysome were each divided into six subcompartments. The limit of the reaction rate as the number of subcompartments increases infinitely is the actual reaction rate, but there was little change in the estimated reaction rate past six subcompartments, so that number of subcompartments was deemed sufficient.

The system of differential equations (Supplemental Appendix S1) was solved by numerical integration using the lsodes algorithm from the deSolve package (Soetaert et al., 2010; version 1.10-4) in the R statistical computing language (R Development Core Team, 2012; version 2.15.2). This algorithm is part of the ODEPACK collection of differential equation solvers and was chosen for its ability to solve stiff sets of equations (Hindmarsh, 1983; Radhakrishnan and Hindmarsh, 1993). The simulation time was 20 s, which was long enough for the system to reach steady state. The maximum time step size was set to 0.02 s, and the relative error tolerance was set to 1×10^{-7}. Source codes to run the model are provided in the supplemental material (Supplemental Data S1 and S2).

Sensitivity was calculated as $\frac{\Delta A_{sat}}{\Delta x} \cdot \frac{x}{A_{sat}}$, where x is the value of the parameter. Although the true sensitivity should be calculated using the derivative $\frac{dA_{sat}}{dx} \cdot \frac{x}{A_{sat}}$, this is not possible here because the equations were solved numerically. Therefore, to estimate the derivative, for each parameter, the model was run three times using the literature value of the parameter (Table I), a value 10% lower than the literature value, and a value 10% higher than the literature value, producing three estimates of A_{sat}. For each parameter, a linear regression was fit to the three resulting points, with the value of the parameter as the dependent variable and A_{sat} as the independent variable. The slope of that fit was used as $\frac{\Delta A_{sat}}{\Delta x}$. For all parameters, a 10% change from the value used in the model was small enough that the response of A_{sat} versus x was linear. Thus, $\frac{\Delta A_{sat}}{\Delta x}$ provided a good estimate of $\frac{dA_{sat}}{dx}$. A similar procedure was used to determine the sensitivity of carboxysomal [CO_2] to parameters in the model using carboxysomal [CO_2] as the independent variable instead of A_{sat}.

To examine the performance of different Rubisco isoforms, kinetics for different isoforms (Supplemental Table S2) were used in a model of a normal C_3 leaf, again with the same leaf but with the complete cyanobacterial CCM added, and with the Rubisco confined to the carboxysome.

To determine the ATP use per net carboxylation, stoichiometries for ATP per HCO_3^- of 1, 0.5, and 0.25 were used for BCT1, SbtA, and BicA, respectively (Price et al., 2011). Net carboxylation by Rubisco was calculated as:

$$v_{c,net} = v_c - \frac{v_o}{2} \quad (11)$$

Supplemental Data

The following materials are available in the online version of this article.

Supplemental Table S1. Modeled A_{sat} using all combinations of cyanobacterial CCM components.

Supplemental Table S2. Kinetic parameters for Rubisco isoforms.

Supplemental Data S1. Model source code.

Supplemental Data S2. The odemodel package for R.

Supplemental Appendix S1. Rate equations.

ACKNOWLEDGMENTS

We thank G. Dean Price for providing data for protein concentrations for NDH1,3 and NDH1,4. The visual table of contents icon was derived from an image created by Todd Yeates.

Received December 13, 2013; accepted February 16, 2014; published February 18, 2014.

LITERATURE CITED

Ainsworth EA, Rogers A, Nelson R, Long SP (2004) Testing the "source-sink" hypothesis of down-regulation of photosynthesis in elevated [CO_2] in the field with single gene substitution in *Glycine max*. Agric For Meteorol **122:** 85–94

Alberty RA (1953) The relationship between Michaelis constants, maximum velocities and the equilibrium constant for an enzyme-catalyzed reaction. J Am Chem Soc **75:** 1928–1932

Baker NR, Long SP, Ort DR (1988) Photosynthesis and temperature, with particular reference to effects on quantum yield. *In* SP Long, FI Woodward, eds, Symposia of the Society for Experimental Biology, Vol 42. Cambridge University Press, Cambridge, UK, pp 347–375

Bernacchi CJ, Kimball BA, Quarles DR, Long SP, Ort DR (2007) Decreases in stomatal conductance of soybean under open-air elevation of [CO_2] are closely coupled with decreases in ecosystem evapotranspiration. Plant Physiol **143:** 134–144

Bernacchi CJ, Leakey ADB, Heady LE, Morgan PB, Dohleman FG, McGrath JM, Gillespie KM, Wittig VE, Rogers A, Long SP, et al (2006) Hourly and seasonal variation in photosynthesis and stomatal conductance of soybean grown at future CO_2 and ozone concentrations for 3 years under fully open-air field conditions. Plant Cell Environ **29:** 2077–2090

Bernacchi CJ, Morgan PB, Ort DR, Long SP (2005) The growth of soybean under free air [CO_2] enrichment (FACE) stimulates photosynthesis while decreasing *in vivo* Rubisco capacity. Planta **220:** 434–446

Bernacchi CJ, Portis AR, Nakano H, von Caemmerer S, Long SP (2002) Temperature response of mesophyll conductance: implications for the determination of Rubisco enzyme kinetics and for limitations to photosynthesis in vivo. Plant Physiol **130:** 1992–1998

Berner T (1993) Ultrastructure of Microalgae. CRC Press, Boca Raton, FL

Burnell JN (2011) Hurdles to engineering greater photosynthetic rates in crop plants: C_4 rice. *In* AS Raghavendra, RF Sage, eds, C_4 Photosynthesis and Related CO_2 Concentrating Mechanisms. Springer, Dordrecht, The Netherlands, pp 361–378

Byott GS (1976) Leaf air space systems in C_3 and C_4 species. New Phytol **76:** 295–299

Cai F, Menon BB, Cannon GC, Curry KJ, Shively JM, Heinhorst S (2009) The pentameric vertex proteins are necessary for the icosahedral carboxysome shell to function as a CO_2 leakage barrier. PLoS ONE **4:** e7521

Covshoff S, Hibberd JM (2012) Integrating C_4 photosynthesis into C_3 crops to increase yield potential. Curr Opin Biotechnol **23:** 209–214

Daughtry CST, Walthall CL, Kim MS, de Colstoun EB, McMurtrey JE III (2000) Estimating corn leaf chlorophyll concentration from leaf and canopy reflectance. Remote Sens Environ **74:** 229–239

David P, Baumann M, Wikström M, Finel M (2002) Interaction of purified NDH-1 from *Escherichia coli* with ubiquinone analogues. Biochim Biophys Acta **1553:** 268–278

Dou Z, Heinhorst S, Williams EB, Murin CD, Shively JM, Cannon GC (2008) CO_2 fixation kinetics of *Halothiobacillus neapolitanus* mutant carboxysomes lacking carbonic anhydrase suggest the shell acts as a diffusional barrier for CO_2. J Biol Chem **283:** 10377–10384

Espie GS, Kimber MS (2011) Carboxysomes: cyanobacterial Rubisco comes in small packages. Photosynth Res **109:** 7–20

Evans JR, Kaldenhoff R, Genty B, Terashima I (2009) Resistances along the CO_2 diffusion pathway inside leaves. J Exp Bot **60:** 2235–2248

FAOSTAT (2013) Food and Agriculture Organization, Rome, Italy. http://faostat.fao.org (December 2, 2013)

Farquhar GD, von Caemmerer S, Berry JA (1980) A biochemical model of photosynthetic CO_2 assimilation in leaves of C_3 species. Planta **149:** 78–90

Gibson JL, Tabita FR (1977) Different molecular forms of D-ribulose-1,5-bisphosphate carboxylase from *Rhodopseudomonas sphaeroides*. J Biol Chem **252:** 943–949

Gillon JS, Yakir D (2000) Internal conductance to CO_2 diffusion and $C^{18}OO$ discrimination in C_3 leaves. Plant Physiol **123:** 201–214

Gutknecht J, Bisson MA, Tosteson FC (1977) Diffusion of carbon dioxide through lipid bilayer membranes: effects of carbonic anhydrase, bicarbonate, and unstirred layers. J Gen Physiol **69:** 779–794

Harrison EP, Olcer H, Lloyd JC, Long SP, Raines CA (2001) Small decreases in SBPase cause a linear decline in the apparent RuBP regeneration rate, but do not affect Rubisco carboxylation capacity. J Exp Bot **52:** 1779–1784

Hindmarsh AC (1983) ODEPACK, a systematized collection of ODE solvers. IMACS Transactions on Scientific Computation **1:** 55–64

Kerfeld CA, Sawaya MR, Tanaka S, Nguyen CV, Phillips M, Beeby M, Yeates TO (2005) Protein structures forming the shell of primitive bacterial organelles. Science **309:** 936–938

Kimball BA, Kobayashi K, Bindi M (2002) Responses of agricultural crops to free-air CO_2 enrichment. Adv Agron **77:** 293–368

Kinney JN, Axen SD, Kerfeld CA (2011) Comparative analysis of carboxysome shell proteins. Photosynth Res **109:** 21–32

Klein MG, Zwart P, Bagby SC, Cai F, Chisholm SW, Heinhorst S, Cannon GC, Kerfeld CA (2009) Identification and structural analysis of a novel carboxysome shell protein with implications for metabolite transport. J Mol Biol **392:** 319–333

Köhler RH, Schwille P, Webb WW, Hanson MR (2000) Active protein transport through plastid tubules: velocity quantified by fluorescence correlation spectroscopy. J Cell Sci **113:** 3921–3930

Larsson S, Björkbacka H, Forsman C, Samuelsson G, Olsson O (1997) Molecular cloning and biochemical characterization of carbonic anhydrase from Populus tremula × tremuloides. Plant Mol Biol **34:** 583–592

Lefebvre S, Lawson T, Zakhleniuk OV, Lloyd JC, Raines CA, Fryer M (2005) Increased sedoheptulose-1,7-bisphosphatase activity in transgenic tobacco plants stimulates photosynthesis and growth from an early stage in development. Plant Physiol **138:** 451–460

Long BM, Badger MR, Whitney SM, Price GD (2007) Analysis of carboxysomes from *Synechococcus* PCC7942 reveals multiple Rubisco complexes with carboxysomal proteins CcmM and CcaA. J Biol Chem **282:** 29323–29335

Long BM, Tucker L, Badger MR, Price GD (2010) Functional cyanobacterial β-carboxysomes have an absolute requirement for both long and short forms of the CcmM protein. Plant Physiol **153:** 285–293

Long SP, Ainsworth EA, Leakey ADB, Nösberger J, Ort DR (2006a) Food for thought: lower-than-expected crop yield stimulation with rising CO_2 concentrations. Science **312:** 1918–1921

Long SP, Ainsworth EA, Rogers A, Ort DR (2004) Rising atmospheric carbon dioxide: plants FACE the future. Annu Rev Plant Biol **55:** 591–628

Long SP, Ort DR (2010) More than taking the heat: crops and global change. Curr Opin Plant Biol **13:** 241–248

Long SP, Zhu XG, Naidu SL, Ort DR (2006b) Can improvement in photosynthesis increase crop yields? Plant Cell Environ **29:** 315–330

Ludwig M, Sültemeyer D, Price GD (2000) Isolation of ccmKLMN genes from the marine cyanobacterium, Synechococcus sp. PCC7002 (Cyanophyceae), and evidence that CcmM is essential for carboxysome assembly. J Phycol **36:** 1109–1119

Maliga P (2004) Plastid transformation in higher plants. Annu Rev Plant Biol **55:** 289–313

Massad RS, Tuzet A, Bethenod O (2007) The effect of temperature on C_4-type leaf photosynthesis parameters. Plant Cell Environ **30:** 1191–1204

Menon BB, Heinhorst S, Shively JM, Cannon GC (2010) The carboxysome shell is permeable to protons. J Bacteriol **192:** 5881–5886

Meyers B, Zaltsman A, Lacroix B, Kozlovsky SV, Krichevsky A (2010) Nuclear and plastid genetic engineering of plants: comparison of opportunities and challenges. Biotechnol Adv **28:** 747–756

Nobel PS (1983) Biophysical Plant Physiology and Ecology. WH Freeman, San Francisco

Omata T, Price GD, Badger MR, Okamura M, Gohta S, Ogawa T (1999) Identification of an ATP-binding cassette transporter involved in bicarbonate uptake in the cyanobacterium *Synechococcus* sp. strain PCC 7942. Proc Natl Acad Sci USA **96:** 13571–13576

Omata T, Takahashi Y, Yamaguchi O, Nishimura T (2002) Structure, function and regulation of the cyanobacterial high-affinity bicarbonate transporter, BCT1. Funct Plant Biol **29:** 151–159

Perez-gago MB, Krochta JM (2001) Denaturation time and temperature effects on solubility, tensile properties, and oxygen permeability of whey protein edible films. J Food Sci **66:** 705–710

Pocker Y, Miksch RR (1978) Plant carbonic anhydrase: properties and bicarbonate dehydration kinetics. Biochemistry **17:** 1119–1125

Pocker Y, Ng SY (1973) Plant carbonic anhydrase: properties and carbon dioxide hydration kinetics. Biochemistry **12:** 5127–5134

Price GD, Badger MR, von Caemmerer S (2011) The prospect of using cyanobacterial bicarbonate transporters to improve leaf photosynthesis in C_3 crop plants. Plant Physiol **155:** 20–26

Price GD, Badger MR, Woodger FJ, Long BM (2008) Advances in understanding the cyanobacterial CO_2-concentrating-mechanism (CCM): functional components, Ci transporters, diversity, genetic regulation and prospects for engineering into plants. J Exp Bot **59:** 1441–1461

Price GD, Howitt SM, Harrison K, Badger MR (1993) Analysis of a genomic DNA region from the cyanobacterium Synechococcus sp. strain PCC7942 involved in carboxysome assembly and function. J Bacteriol **175:** 2871–2879

Price GD, Pengelly JJL, Forster B, Du J, Whitney SM, von Caemmerer S, Badger MR, Howitt SM, Evans JR (2013) The cyanobacterial CCM as a source of genes for improving photosynthetic CO_2 fixation in crop species. J Exp Bot **64:** 753–768

Price GD, von Caemmerer S, Evans JR, Siebke K, Anderson JM, Badger MR (1998) Photosynthesis is strongly reduced by antisense suppression of chloroplastic cytochrome bf complex in transgenic tobacco. Funct Plant Biol **25:** 445–452

Price GD, Woodger FJ, Badger MR, Howitt SM, Tucker L (2004) Identification of a SulP-type bicarbonate transporter in marine cyanobacteria. Proc Natl Acad Sci USA **101:** 18228–18233

Pritchard HW, Grout BWW, Short KC (1986) Osmotic stress as a pregrowth procedure for cryopreservation. 1. Growth and ultrastructure of sycamore and soybean cell suspensions. Ann Bot (Lond) **57:** 41–48

Radhakrishnan K, Hindmarsh AC (1993) Description and Use of LSODE, the Livermore Solver for Ordinary Differential Equations. National Aeronautics and Space Administration, Washington, DC

Rae BD, Long BM, Badger MR, Price GD (2012) Structural determinants of the outer shell of β-carboxysomes in Synechococcus elongatus PCC 7942: roles for CcmK2, K3-K4, CcmO, and CcmL. PLoS ONE **7:** e43871

Raven JA, Allen JF (2003) Genomics and chloroplast evolution: what did cyanobacteria do for plants? Genome Biol **4:** 209

Ray DK, Ramankutty N, Mueller ND, West PC, Foley JA (2012) Recent patterns of crop yield growth and stagnation. Nat Commun **3:** 1293

Rosenthal DM, Locke AM, Khozaei M, Raines CA, Long SP, Ort DR (2011) Over-expressing the C_3 photosynthesis cycle enzyme sedoheptulose-1-7 bisphosphatase improves photosynthetic carbon gain and yield under fully open air CO_2 fumigation (FACE). BMC Plant Biol **11:** 123

Ruuska SA, Andrews TJ, Badger MR, Price GD, von Caemmerer S (2000) The role of chloroplast electron transport and metabolites in modulating Rubisco activity in tobacco: insights from transgenic plants with reduced amounts of cytochrome b/f complex or glyceraldehyde 3-phosphate dehydrogenase. Plant Physiol **122:** 491–504

Scalettar BA, Abney JR, Hackenbrock CR (1991) Dynamics, structure, and function are coupled in the mitochondrial matrix. Proc Natl Acad Sci USA **88:** 8057–8061

Sheehy JE, Dionora MJA, Mitchell PL (2001) Spikelet numbers, sink size and potential yield in rice. Field Crops Res **71:** 77–85

Shibata M, Katoh H, Sonoda M, Ohkawa H, Shimoyama M, Fukuzawa H, Kaplan A, Ogawa T (2002) Genes essential to sodium-dependent bicarbonate

transport in cyanobacteria: function and phylogenetic analysis. J Biol Chem **277:** 18658–18664

Slaton M R, Smith W K (2002) Mesophyll architecture and cell exposure to intercellular air space in alpine, desert, and forest species. Int J Plant Sci **163:** 937–948

Slewinski TL (2013) Using evolution as a guide to engineer Kranz-type C_4 photosynthesis. Front Plant Sci **4:** 212

Soetaert K, Petzoldt T, Setzer RW (2010) Solving differential equations in R: package deSolve. J Stat Softw **33:** 9

R Development Core Team (2012) R: A Language and Environment for Statistical Computing. R Foundation for Statistical Computing, Vienna

Terashima I, Hanba YT, Tholen D, Niinemets Ü (2011) Leaf functional anatomy in relation to photosynthesis. Plant Physiol **155:** 108–116

Tholen D, Zhu XG (2011) The mechanistic basis of internal conductance: a theoretical analysis of mesophyll cell photosynthesis and CO_2 diffusion. Plant Physiol **156:** 90–105

Tomás M, Flexas J, Copolovici L, Galmés J, Hallik L, Medrano H, Ribas-Carbó M, Tosens T, Vislap V, Niinemets Ü (2013) Importance of leaf anatomy in determining mesophyll diffusion conductance to CO_2 across species: quantitative limitations and scaling up by models. J Exp Bot **64:** 2269–2281

von Caemmerer S (2000) Biochemical Models of Leaf Photosynthesis. CSIRO Publishing, Collingwood, Australia

Winter H, Robinson DG, Heldt HW (1994) Subcellular volumes and metabolite concentrations in spinach leaves. Planta **193:** 530–535

Wullschleger SD (1993) Biochemical limitations to carbon assimilation in C_2 plants: a retrospective analysis of the A/Ci curves from 109 species. J Exp Bot **44:** 907–920

Yeates TO, Kerfeld CA, Heinhorst S, Cannon GC, Shively JM (2008) Protein-based organelles in bacteria: carboxysomes and related microcompartments. Nat Rev Microbiol **6:** 681–691

Yeates TO, Thompson MC, Bobik TA (2011) The protein shells of bacterial microcompartment organelles. Curr Opin Struct Biol **21:** 223–231

Yu W, Long SP, Zhu XG (2014) Elements required for an efficient NADP-ME type C4 photosynthesis: exploration using a systems model of C4 photosynthesis. Plant Physiol (in press)

Zhu XG, de Sturler E, Long SP (2007) Optimizing the distribution of resources between enzymes of carbon metabolism can dramatically increase photosynthetic rate: a numerical simulation using an evolutionary algorithm. Plant Physiol **145:** 513–526

Zhu XG, Long SP, Ort DR (2010) Improving photosynthetic efficiency for greater yield. Annu Rev Plant Biol **61:** 235–261

Zhu XG, Wang Y, Ort DR, Long SP (2013) E-photosynthesis: a comprehensive dynamic mechanistic model of C_3 photosynthesis: from light capture to sucrose synthesis. Plant Cell Environ **36:** 1711–1727